

Nonperturbative model for optical response under intense periodic fields with application to graphene in a strong perpendicular magnetic field

J. L. Cheng^{1,2} and C. Guo^{1,3}

¹*The Guo China-US Photonics Laboratory, Changchun Institute of Optics, fine Mechanics and Physics, Chinese Academy of Sciences, 3888 Eastern South Lake Road, Changchun, Jilin 130033, China.*

²*University of Chinese Academy of Sciences, Beijing 100049, China*

³*The Institute of Optics, University of Rochester, Rochester, NY 14627, USA.*

(Dated: September 20, 2018)

Graphene exhibits extremely strong optical nonlinearity when a strong perpendicular magnetic field is applied, the response current shows strong field dependence even for moderate light intensity, and the perturbation theory fails. We nonperturbatively calculate full optical conductivities induced by a periodic field in an equation-of-motion framework based on the Floquet theorem, with the scattering described phenomenologically. The nonlinear response at high fields is understood in terms of the dressed electronic states, or Floquet states, which is further characterized by the optical conductivity for a weak probe light field. This approach is illustrated for a magnetic field at 5 T and a driving field with photon energy 0.05 eV. Our results show that the perturbation theory works only for weak fields < 3 kV/cm, confirming the extremely strong light matter interaction for Landau levels of graphene. This approach can be easily extended to the calculation of optical conductivities in other systems.

I. INTRODUCTION

Landau levels (LLs) of graphene show unique properties including a large cyclotron energy $\hbar\omega_c \approx 36\sqrt{B}$ (Tesla) meV and nonequidistant energies. This suggests that graphene in a strong magnetic field should be a good platform for demonstrating many fundamental dynamics concepts,¹ even at room temperature. Recent studies of the nonlinear responses have been extended to wavelengths in the infrared.²⁻⁷ A huge optical susceptibility is predicted by Yao and Belyanin^{3,4} and confirmed by the four wave mixing (FWM) experiments of König-Otto *et al.* in the far infrared.⁵ Proposed applications for graphene-based photonics include the generation of entangled photons,⁸ an all-optical switch,⁹ tunable lasers,⁶ the dynamic control of coherent pulses,¹⁰ and the demonstration of optical bistability and optical multistability.^{11,12}

Theoretically, optical nonlinearities are mostly studied in an equation-of-motion framework, where solutions of the dynamical equations can be obtained in the rotating wave approximation (RWA)^{3,4} or in perturbation method.⁷ RWA is suitable for resonant transitions and modest incident laser intensities, which are usually discussed between lowest several LLs. The perturbation theory can easily include the contribution from all LLs, and it works well only for weak light intensities. However, both theoretical prediction³ and experimental measurement⁵ confirm that the LLs of graphene have a very weak saturation fields with values around a few kV/cm. For high fields, the optical response could be obtained by numerical simulation, but often such calculations do not lead to physical insight into the underlying physics. In this paper, we propose to investigate the nonlinear response in the basis of Floquet states.

When electrons are driven by a periodic field at fre-

quency Ω , the electronic states can be expressed by Floquet theorem¹³ as Floquet states, which are nonperturbative solution of Schrödinger equation with light matter interaction. This approach is used to study the gap opening by a laser field in graphene¹⁴⁻¹⁶ and Floquet topological insulators.¹⁷ For graphene in the absence of magnetic fields, it has also been applied to study the transport and linear optical properties,¹⁸⁻²¹ the dynamic Franz-Keldysh effect,^{19,22} and side band effects.¹⁹ Recently, Kibis *et al.*²³ used Floquet theorem to study the optical and transport effects of dressed LLs of graphene by a monochromatic field. When there is adequate damping, the system can reach a steady state that is also periodic in time and can be probed²⁴ by a weak light with a different frequency ω . Generally, the response current includes components at frequencies $l\Omega$ and $l\Omega + \omega$ with integer l . Most studies focus on the response current components at frequencies Ω and ω ; few discussion is performed for components at other frequencies, which are essential quantities for many nonlinear optical phenomena including third harmonic generation (THG) and FWM.

In this paper we extend the Floquet theorem to study optical nonlinearity in the equation-of-motion framework under relaxation time approximation, and set up a connection between the obtained expressions and the perturbation results. We apply this approach to the optical response of LLs of graphene. Due to the strong light matter interaction, this approach is illustrated for field below a few tens kV/cm, which can be generated by continuous wave laser or long duration laser pulse. For considered field strength, the relaxation time approximation is still a widely used description³ for scattering. As such, we discuss the nonlinear response including THG and FWM.

We organize the paper as follows. In Sec. II we give all the expression for the response currents and conduc-

tivities from a general point of view; in Sec. III we apply the model to graphene under a strong perpendicular magnetic field, and show the optical nonlinearities for its steady state and the probe conductivities when a probe field is introduced; in Sec. IV we conclude and discuss the possible issue to be fixed in the future.

II. METHOD

We consider optical response of a N -level system (states labeled by Roman letters $n = 1, 2, \dots, N$) to an electric field $\mathbf{E}(t)$. The Hamiltonian can be written as

$$\hat{H}(t) = \hat{H}_0 + e\theta(t)\mathbf{E}(t) \cdot \hat{\boldsymbol{\xi}}, \quad (1)$$

where $-e$ is the electron charge, \hat{H}_0 is the unperturbed Hamiltonian described by a $N \times N$ matrix with elements $(\hat{H}_0)_{mn} = \varepsilon_m \delta_{mn}$, and $\hat{\boldsymbol{\xi}}$ is a matrix describing the dipole interaction. A quantity with a hat \hat{O} stands for a matrix with row and column indexed by the level index n . The electric field $\mathbf{E}(t) = \mathbf{E}_{\text{drv}}(t) + \mathbf{E}_{\text{prb}}(t)$ includes a driving field $\mathbf{E}_{\text{drv}}(t)$, which can be strong, and a probe field $\mathbf{E}_{\text{prb}}(t)$, which is usually very weak. The light-matter interaction is turned on at $t = 0$ suddenly. The time evolution of the system is described by the equation of motion

$$\hbar \frac{\partial \hat{\rho}(t)}{\partial t} = -i[\hat{H}(t), \hat{\rho}(t)] - \hbar\gamma[\hat{\rho}(t) - \hat{\rho}^0], \quad (2)$$

where $\hat{\rho}(t)$ is a single-particle density matrix. The last term is a widely used phenomenological description of the scattering, with $\hat{\rho}^0$ the density matrix at equilibrium state and γ a relaxation parameter. We organize the formal solution as

$$\hat{\rho}(t) = \hat{\rho}^0 + \hat{\rho}_{\text{drv}}(t) + \hat{\rho}_{\text{prb}}(t), \quad (3)$$

$$\hat{\rho}_{\text{drv}}(t) = \frac{e}{i\hbar} \int_0^t d\tau e^{\gamma(\tau-t)} \hat{U}(t, \tau) \mathbf{E}_{\text{drv}}(\tau) \cdot [\hat{\boldsymbol{\xi}}, \hat{\rho}^0] \hat{U}(\tau, t), \quad (4)$$

$$\hat{\rho}_{\text{prb}}(t) = \frac{e}{i\hbar} \int_0^t d\tau e^{\gamma(\tau-t)} \hat{U}(t, \tau) \mathbf{E}_{\text{prb}}(\tau) \cdot [\hat{\boldsymbol{\xi}}, \hat{\rho}(\tau)] \hat{U}(\tau, t) \quad (5)$$

where $\hat{U}(t, \tau) = \sum_{\alpha} \psi_{\alpha}(t) \psi_{\alpha}^{\dagger}(\tau)$ is an unitary matrix, and $\psi_{\alpha}(t)$ satisfies the Schrödinger equation

$$i\hbar \partial_t \psi_{\alpha}(t) = [\hat{H}_0 + e\mathbf{E}_d(t) \cdot \hat{\boldsymbol{\xi}}] \psi_{\alpha}(t), \quad \text{for } t > 0. \quad (6)$$

Because we are only interested in the solution at $t > 0$, the factor $\theta(t)$ appearing in the Hamiltonian $H(t)$ can be ignored. Here the Greek subscript α stands for the index of the eigenstate with the inclusion of the driving field. Obviously, the unitary matrix satisfies $\hat{U}(\tau, \tau) = I$. We are interested in the response current density⁷ $\mathbf{J}(t) = -e\text{Tr}[\hat{\mathbf{v}}\hat{\rho}(t)]$ with $\hat{\mathbf{v}} = [\hat{\boldsymbol{\xi}}, \hat{H}(t)]/(i\hbar) = [\hat{\boldsymbol{\xi}}, \hat{H}_0]/(i\hbar)$. Further we can write it as $\mathbf{J}(t) = \mathbf{J}_{\text{drv}}(t) + \mathbf{J}_{\text{prb}}(t)$, where the driving current is $\mathbf{J}_{\text{drv}}(t) = -e\text{Tr}[\hat{\mathbf{v}}\hat{\rho}_{\text{drv}}(t)]$ and the probe current $\mathbf{J}_{\text{prb}}(t) = -e\text{Tr}[\hat{\mathbf{v}}\hat{\rho}_{\text{prb}}(t)]$.

Here we consider a special driving field, which is periodic

$$\mathbf{E}_{\text{drv}}^d(t) = \sum_l \mathbf{E}_{\text{drv}}^{(l);d} e^{-il\Omega t}, \quad (7)$$

where the Roman superscripts stand for the Cartesian directions $\hat{\mathbf{x}}$ or $\hat{\mathbf{y}}$. Using the Floquet theorem,¹³ the eigen states are Floquet states, which are dressed electronic states and can be expanded as

$$\psi_{\alpha}(t) = e^{-i\epsilon_{\alpha}t/\hbar} \sum_l e^{-il\Omega t} u_{\alpha}^{(l)}, \quad (8)$$

where ϵ_{α} is the quasi-energy, $u_{\alpha}^{(l)}$ is a N -row vector, and $\{u_{\alpha}^{(l)}, l = \dots, -1, 0, 1, \dots\}$ forms the α th eigen vectors. They satisfy the eigen equation

$$(l\hbar\Omega + \epsilon_{\alpha})u_{\alpha}^{(l)} = \hat{H}_0 u_{\alpha}^{(l)} + \sum_n e\mathbf{E}_{\text{drv}}^{(n);d} \hat{\boldsymbol{\xi}}^d u_{\alpha}^{(l-n)}. \quad (9)$$

Although $\{u_{\alpha}^{(l+m)}, l = \dots, -1, 0, 1, \dots\}$ for any integer m is also an eigenstate of Eq. (9) with energy $\epsilon_{\alpha} + m\hbar\Omega$, they correspond to the same state $\psi_{\alpha}(t)$ of the Schrödinger equation (6); only one of them needs to be considered. The normalization of $\psi_{\alpha}(t)$ in Eq. (8) gives $\text{Tr}[\hat{\mathcal{A}}_{\alpha_1\alpha_2}^{(l)}] = \delta_{\alpha_1\alpha_2} \delta_{l,0}$ with $\hat{\mathcal{A}}_{\alpha_1\alpha_2}^{(l)} = \sum_{l_1} u_{\alpha_2}^{(l_1)} [u_{\alpha_1}^{(l-l_1)}]^{\dagger}$. After some algebra, we get

$$\hat{\rho}_{\text{drv}}(t) = \sum_l e^{-il\Omega t} \hat{\rho}_{\text{drv}}^{(l)}(t), \quad (10)$$

$$\hat{\rho}_{\text{drv}}^{(l)}(t) = \sum_{\alpha_1\alpha_2 l_1} \mathcal{A}_{\alpha_2\alpha_1}^{(l_1)} G_{\alpha_1\alpha_2}^{(l-l_1)} \times [1 - e^{-\gamma t} e^{i(l-l_1)\Omega t} e^{-i(\epsilon_{\alpha_1} - \epsilon_{\alpha_2})t/\hbar}], \quad (11)$$

$$G_{\alpha_1\alpha_2}^{(l)} = \frac{e \sum_{l_2} E_{\text{drv}}^{(l_2);d} \text{Tr} \left\{ [\hat{\boldsymbol{\xi}}^d, \hat{\rho}^0] \hat{\mathcal{A}}_{\alpha_1\alpha_2}^{(l-l_2)} \right\}}{l\hbar\Omega - (\epsilon_{\alpha_1} - \epsilon_{\alpha_2}) + i\hbar\gamma}. \quad (12)$$

Here $\hat{\rho}_{\text{drv}}^{(l)}(t)$ includes oscillating terms related to the correlations between Floquet states, but decaying with a factor $e^{-\gamma t}$. These oscillations correspond to damped Rabi oscillations. As $t \rightarrow \infty$, they vanish, then $\hat{\rho}_{\text{drv}}^{(l)}(t)$ and $\hat{\rho}_{\text{drv}}(t)$ reach their steady state, which are also periodic in time. In the clean limit $\gamma \rightarrow 0$, an apparent divergence appears in the expression of $G_{\alpha\alpha}^{(0)}$, which can be shown to vanish from Eq. (9).²⁵ This is not surprising because our results are the full solutions of Schrödinger equation, which should not diverge. The asymptotic current as $t \rightarrow \infty$ is

$$\mathbf{J}_{\text{drv}}^d(t \rightarrow \infty) = \sum_l e^{-il\Omega t} \mathbf{J}_{\text{drv}}^{(l);d}, \quad (13)$$

$$\mathbf{J}_{\text{drv}}^{(l);d} = -e \sum_{\alpha_1\alpha_2 l_1} v_{\alpha_2\alpha_1}^{(l_1);d} G_{\alpha_1\alpha_2}^{(l-l_1)}. \quad (14)$$

Here we used notation $\text{Tr}[\hat{X} \hat{\mathcal{A}}_{\alpha_1\alpha_2}^{(l)}] = X_{\alpha_1\alpha_2}^{(l)}$ for $\hat{X} = \hat{v}^d$.

The effects induced by the driving field can also be detected by a probe light $\mathbf{E}_{\text{prb}}(t)$. It leads to a change

of the density matrix by $\hat{\rho}_{\text{prb}}(t)$, and induces a probe current density $\mathbf{J}_{\text{prb}}(t)$. Up to the linear order of \mathbf{E}_{prb} , we solve $\hat{\rho}_{\text{prb}}(t)$ in Eq. (5) by setting $\hat{\rho}(\tau) = \hat{\rho}^0 + \hat{\rho}_{\text{drv}}(\tau)$ and take the asymptotic results as $t \rightarrow \infty$ to give

$$\hat{\rho}_{\text{prb}}(t \rightarrow \infty) = \int \frac{d\omega}{2\pi} \sum_l e^{-i\Omega t - i\omega t} e E_p^b(\omega) \sum_{\alpha_1 \alpha_2 l_1} \hat{\mathcal{A}}_{\alpha_2 \alpha_1}^{(l_1)} \times \left[\mathcal{G}_{\alpha_1 \alpha_2}^{(l-1);b}(\omega) + \mathcal{P}_{\alpha_1 \alpha_2}^{(l-1);b}(\omega) \right], \quad (15)$$

with

$$\mathcal{G}_{\alpha_1 \alpha_2}^{(l);b}(\omega) = \frac{\text{Tr} \left\{ \left[\hat{\xi}^b, \hat{\rho}^0 \right] \hat{\mathcal{A}}_{\alpha_1 \alpha_2}^{(l)} \right\}}{l\hbar\Omega + \hbar\omega - (\epsilon_{\alpha_1} - \epsilon_{\alpha_2}) + i\hbar\gamma}, \quad (16)$$

$$\mathcal{P}_{\alpha_1 \alpha_2}^{(l);b}(\omega) = \frac{\sum_{\alpha l_2} \left[\xi_{\alpha_1 \alpha}^{(l-1);b} G_{\alpha \alpha_2}^{(l_2)} - G_{\alpha_1 \alpha}^{(l_2)} \xi_{\alpha \alpha_2}^{(l-1);b} \right]}{l\hbar\Omega + \hbar\omega - (\epsilon_{\alpha_1} - \epsilon_{\alpha_2}) + i\hbar\gamma} \quad (17)$$

Here the term \mathcal{G} is from $\hat{\rho}^0$, and the term \mathcal{P} is from $\hat{\rho}_{\text{drv}}$. The current density is then

$$\mathbf{J}_{\text{prb}}^d(t \rightarrow \infty) = \int \frac{d\omega}{2\pi} \sum_l e^{-i(l\Omega + \omega)t} \sigma_{\text{prb}}^{(l);db}(\omega) E_{\text{prb}}^b(\omega),$$

with the probe conductivity

$$\sigma_{\text{prb}}^{(l);db}(\omega) = -e^2 \sum_{\alpha_1 \alpha_2 l_1} v_{\alpha_2 \alpha_1}^{(l-1);d} \left[\mathcal{G}_{\alpha_1 \alpha_2}^{(l_1);b}(\omega) + \mathcal{P}_{\alpha_1 \alpha_2}^{(l_1);b}(\omega) \right]. \quad (18)$$

The quantities $J_{\text{drv}}^{(l);d}$ and $J_{\text{prb}}^{(l);d}(\omega)$ are experimental observable quantities, which can be extracted by measuring the light intensity of the electromagnetic radiation at frequencies $l\Omega$ and $l\Omega + \omega$, respectively. The driving field affects the probe conductivities in two aspects: One is the energy spectrum of quasi-states, which appear in the denominators of Eqs. (16) and (17). In the limit of weak relaxation, this contribution is significant around resonant peaks. The other is that the steady states of density matrix, including both the occupations at each quasi-state and the polarization between them, are changed by the driving field. The latter dominates the cases away from the resonance.

It is constructive to connect our results with the usual perturbative conductivities. Here the order l in both $J_{\text{drv}}^{(l);d}$ and $\sigma_{\text{prb}}^{(l);db}(\omega)$ correspond to the response frequency $l\Omega$ and $l\Omega + \omega$, respectively, instead of the orders of the driving field. At a weak field, Eq. (9) can be solved perturbatively by treating the last term as a perturbation. In the lowest order with taking $\epsilon_\alpha \rightarrow \epsilon_n = \epsilon_n$ and $X_{\alpha_1 \alpha_2}^{(l)} \rightarrow X_{n_1 n_2}^{(l)} = X_{n_1 n_2} \delta_{l,0}$, $J_{\text{drv}}^{(1);d}$ reduces to the perturbation results.⁷ In general, the remarkable differences come from the denominator of Eqs. (12) and (17). In the limit $\gamma \rightarrow 0$, the absorption edge can be changed by the field, which leads to the so called dynamic Franz-Keldysh effects.²² For a finite γ , in the regime where perturbation theory works, this phenomenon may be smeared out. Usually, the conductivities with the contribution from $l\hbar\Omega$ may be discussed in the content of side-band effects. As we will show later, they can be associated with the nonlinear responses for weak driving field.

III. RESULTS

We apply this approach to graphene in a strong magnetic field, $\mathbf{B} = B\hat{z}$. The electronic states are LLs noted as $|\nu snk\rangle$, where $\nu = + (-)$ is a valley index for the \mathbf{K} (\mathbf{K}') valley, $s = \pm$ is a band index, $n \geq (1 + \nu s)/2$ is a Landau index, and k is a continuum index. The eigen energies are $E_{\nu sn} = s\varepsilon_n$, where with $\varepsilon_n = \sqrt{n}\hbar\omega_c$ with $\hbar\omega_c = \sqrt{2}\hbar v_F/l_c$ and the magnetic length $l_c = \sqrt{\hbar/(eB)}$, which depends on the index “ sn ” only. The continuum index k gives a degeneracy $\mathcal{D} = g_s/(2\pi l_c^2)$ with $g_s = 2$ for spin degeneracy, and this index will be suppressed hereafter. There is no coupling between the two valleys, and the matrix elements of position and velocity operators in the ν th valley can be written as $\xi_{\nu; s_1 n_1, s_2 n_2} = \sum_{\tau=\pm} \xi_{\nu; s_1 n_1, s_2 n_2}^{\tau} (\hat{x} - i\tau\hat{y})/\sqrt{2}$ and $\mathbf{v}_{\nu; s_1 n_1, s_2 n_2} = i\hbar^{-1}(s_1 \varepsilon_{n_1} - s_2 \varepsilon_{n_2}) \xi_{\nu; s_1 n_1, s_2 n_2}$. Inversion symmetry connects the quantities in the two valleys according to $\xi_{+; s_1 n_1, s_2 n_2} = s_1 s_2 \xi_{-; (-s_1) n_1, (-s_2) n_2}$. Considering the Hermiticity of these quantities, all relevant matrix elements can be generated from $v_{+; s_1 n_1, s_2 n_2}^+ = s_1 v_F \delta_{n_1, n_2+1} (\delta_{n_2 \neq 0}/\sqrt{2} + \delta_{n_2, 0} \delta_{s_2, -1})$.

In our calculations, the parameters are taken as $B = 5$ T, $\hbar\Omega = 0.05$ eV, the chemical potential $\mu = 0$ eV, the temperature $T = 10$ K, and $\hbar\gamma = 10$ meV. The driving field is $\mathbf{E}_{\text{drv}}^{(l)} = E_0 \hat{x} (\delta_{l,1} + \delta_{l,-1})$, and the density matrix at equilibrium is $\rho_{\nu; s_1 n_1, s_2 n_2}^0 = [1 + e^{(s_1 \varepsilon_{n_1} - \mu)/(k_B T)}]^{-1} \delta_{s_1 s_2} \delta_{n_1 n_2}$ with k_B the Boltzmann constant. The calculated Floquet states $\psi_\alpha(t)$ in the ν valley is denoted as $|\nu\alpha\rangle_f$ with $\alpha = -N_c, -N_c + 1, \dots, N_c - 1, N_c$ and $N_c = 20$ being the cutoff of Landau index, and their quasi-energies are noted as $\epsilon_{\nu\alpha}$. The driving field is taken as $E_0 < 60$ kV/cm, in which our results are converged for the specified N_c . The energies of the lowest several LLs are $\varepsilon_n = 0, 81, \text{ and } 115$ meV for $n = 0, 1, 2$, respectively. The driving photon energy does not match any of the resonant conditions.

For a linearly polarized field, the system retains the electron-hole symmetry, and thus we can choose the quasi-energy of the Floquet states to satisfy $\epsilon_{\nu\alpha} = -\epsilon_{\nu(-\alpha)}$, and $\epsilon_{\nu 0} = 0$; the occupation $[\hat{\rho}_{\text{drv}}^{(l)}]_{\nu; sn, sn}$ at the LL $|\nu sn\rangle$ also satisfies $[\hat{\rho}_{\text{drv}}^{(l)}]_{\nu; +n, +n} = -[\hat{\rho}_{\text{drv}}^{(l)}]_{\nu; -n, -n}$ and $[\hat{\rho}_{\text{drv}}^{(l)}]_{\nu; -0, -0} = 0$. Furthermore, due to the crystal symmetry, the current responses $J_{\text{drv}}^{(l);d}$ and $\sigma_{\text{prb}}^{(l);db}(\omega)$ are nonzero only for odd order of l , and the density matrix $\rho_{\text{drv}}^{(l)}(t)$ is nonzero only for even order of l . For a comparison with our previous work,⁷ we denote the perturbative conductivities as $\sigma_{\text{pert}}^{(n)}$. In this paper, the relevant conductivities are $\sigma_{\text{pert}}^{(1);xx}(\Omega)$ and $\sigma_{\text{pert}}^{(3);xxxx}(\Omega, \Omega, \pm\Omega)$ for the driving field, and $\sigma_{\text{pert}}^{(3);xxxx}(\Omega, \pm\Omega, \omega)$ for the probe field.

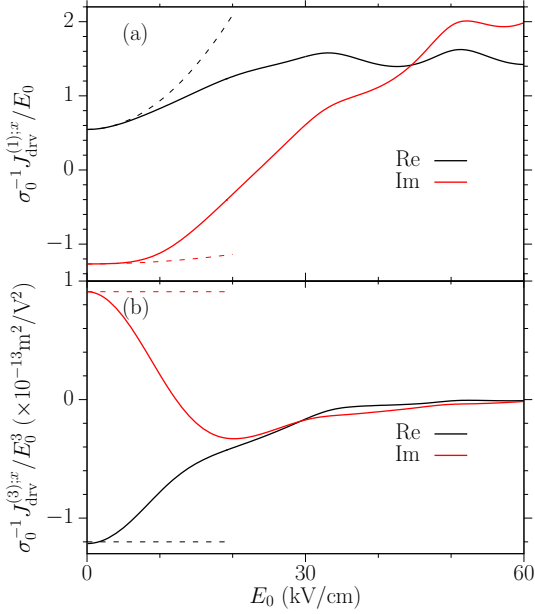


FIG. 1. (color online) Current density induced by the periodic driving field for $E_0 \leq 60$ kV/cm. (a) The effective linear conductivity. (b) The effective conductivity for THG. The dashed curves are perturbation results given in the right hand side of Eqs. (19) and (20).

A. Current density response to the driving field

In Fig. 1 we plot the effective conductivity $\sigma_{\text{eff}}^{(1)} = J_{\text{drv}}^{(1);x}/E_0$ at fundamental frequency Ω and $\sigma_{\text{eff}}^{(3)} = J_{\text{drv}}^{(3);x}/E_0^3$ at the third harmonic frequency 3Ω as a function of the field amplitude E_0 . We first compare these results with perturbation theory to determine the field threshold. At weak field, up to the third order conductivities the effective conductivities are expanded as

$$\sigma_{\text{eff}}^{(1)} \approx \sigma_{\text{pert}}^{(1);xx}(\Omega) + 3\sigma_{\text{pert}}^{(3);xxxx}(\Omega, \Omega, -\Omega)E_0^2, \quad (19)$$

$$\sigma_{\text{eff}}^{(3)} \approx \sigma_{\text{pert}}^{(3);xxxx}(\Omega, \Omega, \Omega). \quad (20)$$

The perturbation results give $\sigma_0^{-1}\sigma_{\text{pert}}^{(1);xx} = 0.55 - 1.27i$ with $\sigma_0 = e^2/(4\hbar)$, $\sigma_0^{-1}\sigma_{\text{pert}}^{(3);xxxx}(\Omega, \Omega, -\Omega) = (0.128 + 0.0108i) \times 10^{-12} \text{ m}^2/\text{V}^2$, and $\sigma_0^{-1}\sigma_{\text{pert}}^{(3);xxxx}(\Omega, \Omega, \Omega) = (-1.2 + 0.91i) \times 10^{-13} \text{ m}^2/\text{V}^2$; they are plotted in Fig. 1 (a) as dashed curves. The perturbation results agree with the full calculation very well when the field is $E_0 < 5$ kV/cm (for $\sigma_{\text{eff}}^{(1)}$) or $E_0 < 3$ kV/cm (for $\sigma_{\text{eff}}^{(3)}$) with an error less than 5%. These small thresholds indicate extremely strong interaction between the periodic field and the LLs of graphene. For large E_0 , the real part of $\sigma_{\text{eff}}^{(1)}$ increases with the field with a slope slower than the perturbation results, and reaches a peak with value $1.58\sigma_0$ at $E_0 \sim 33$ kV/cm; then it shows one oscillation and arrives at another peak at $E_0 \sim 51$ kV/cm. The imaginary part of $\sigma_{\text{eff}}^{(1)}$ firstly increases with the field by a

larger slope, reaches a peak around $E_0 \sim 51$ kV/cm. At $E_0 \sim 33$ kV/cm, the imaginary part shows a shoulder-like fine structure. From our discussion in Sec. II, we can understand these features from the properties of Floquet states.

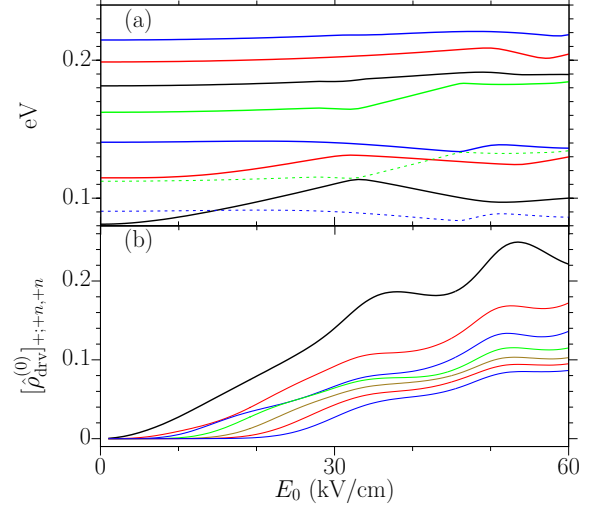


FIG. 2. (color online) (a) Field dependence of quasi-energies $\epsilon_{+\alpha}$ in the \mathbf{K} valley for $1 \leq \alpha \leq 7$. The two dashed curves corresponds to the energy $\epsilon_{+\alpha} - \hbar\Omega$ for $\alpha = 3$ and 4. (b) Field dependence of the zeroth order occupations at different LLs $|++n\rangle$ for $1 \leq n \leq 7$.

In Fig. 2 (a) we plot the field dependence of the quasi-energies $\epsilon_{+\alpha}$ for states $|+\alpha\rangle_f$ in the \mathbf{K} valley for $1 \leq \alpha \leq 7$. At zero field, these states correspond to the LLs $|++n\rangle$ for $1 \leq n \leq 7$. From electron-hole symmetry we can obtain their opposite energy counterparts $\epsilon_{+\alpha} = -\epsilon_{+(-\alpha)}$ and $\epsilon_{+0} = 0$. We focus on the quasi-state $|+1\rangle_f$, which corresponds to the LL $|++1\rangle$ at zero field. Its quasi-energy shows a complicated dependence of E_0 . It starts with 81 meV at zero field, and reaches a local maximum around 113.5 meV at about $E_0 = 33$ kV/cm, then decreases to a local minimum with values 97 meV at $E_0 = 51$ kV/cm, and increases again. For small field, the energy corrections come mostly from the LLs $|+-0\rangle$ and $|+s2\rangle$, due to the selection rules.

For stronger field, the Floquet states mix more LLs; the selection rules between Floquet states can be greatly modified from those between LLs. As an example, we analyze the behavior of the state $|+1\rangle_f$ around $E_0 \sim 33$ kV/cm. The energy of this Floquet state is close to that of $|+4\rangle_f$, which is shown in the same diagram by plotting an equivalent quasi-energy $\epsilon_{+4} - \hbar\Omega$ as a dashed curve. Their interaction is allowed and leads to an anti-crossing (about 1 meV splitting). Similar behavior occurs around the local minimum at $E_0 \sim 51$ kV/cm, which is induced by the interaction between the quasi-states $|+1\rangle_f$ and $|+3\rangle_f$. Besides the modification of the selection rules, the strong field can also greatly change the occupations on each LL, as shown in Figure 2 (b) for the occupation $[\hat{\rho}_{\text{drv}}^{(0)}(t \rightarrow \infty)]_{+;+n,+n}$ of the LL $|+sn\rangle$ for

$1 \leq n \leq 7$. When $E_0 > 30$ kV/cm, the occupation at the LL $|+1\rangle$ is about 0.2, significantly deviating from its thermal equilibrium (~ 0). Therefore, both the quasi-energies and the populations show similar tendencies as the optical conductivity $\sigma_{\text{eff}}^{(1)}$, and they dominate the optical response induced by the driven field, as we discussed in Sec. II. This partly explains why the perturbation theory based on the thermal equilibrium fails.

In Fig. 1 (b) we give the field dependence of the optical conductivity $\sigma_{\text{eff}}^{(3)}$ for THG. Both the real and imaginary parts of $\sigma_{\text{eff}}^{(3)}$ decrease quickly to very small values, and the imaginary part shows a valley around $E_0 \sim 20$ kV/cm. Similar to the $\sigma_{\text{eff}}^{(1)}$, $\sigma_{\text{eff}}^{(3)}$ are mainly affected by the changes of optically excited populations. Because there is no specific physical process to distinguish its real and imaginary parts, they behave in a similar way.

B. Probe conductivities

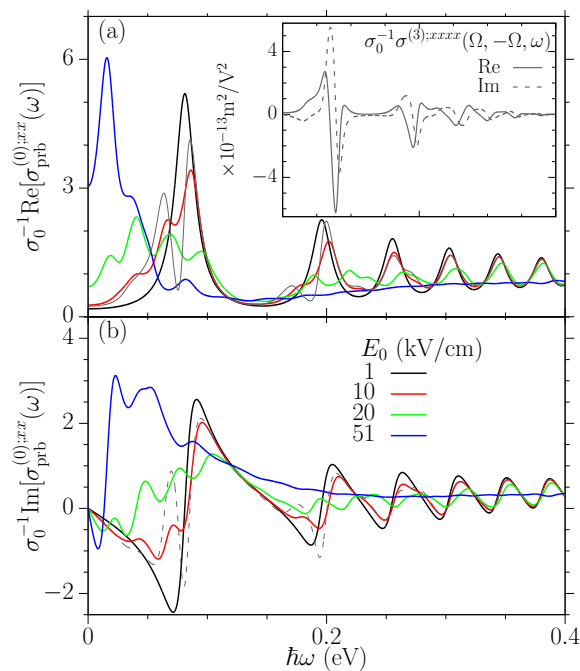


FIG. 3. (color online) The spectrum of the probe conductivity $\sigma_{\text{prb}}^{(0);xx}(\omega)$ for different driving fields with (a) the real part (b) the imaginary part. The inset in (a) shows the perturbative third order conductivity⁷ $\sigma_{\text{pert}}^{(3);xxxx}(\Omega, -\Omega, \omega)$ with x -axis also in $\hbar\omega \in [0, 0.4]$ eV. The gray curves in (a) and (b) are the perturbative probe conductivity up to the third order for $E_0 = 10$ kV/cm.

The modification of the intense field on the LLs can also be probed by a weak optical field. Similarly, for a very weak driving field, the probe conductivities in Eq. (18) can be approximated from perturbation theory,

and up to the third order we have

$$\sigma_{\text{prb}}^{(0);xx}(\omega) \approx \sigma_{\text{pert}}^{(1);xx}(\omega) + 6\sigma_{\text{pert}}^{(3);xxxx}(\Omega, -\Omega, \omega)E_0^2, \quad (21)$$

Here $\sigma_{\text{pert}}^{(1);xx}(\omega)$ and $\sigma_{\text{pert}}^{(3);xxxx}(\Omega, -\Omega, \omega)$ are the perturbative conductivities calculated from our previous work.⁷ In Fig. 3 we give the probe conductivity $\sigma_{\text{prb}}^{(0);xx}(\omega)$ for a probe frequency ω . The calculation at weak field $E_0 = 1$ kV/cm agrees with the perturbation results very well, and the real part show many absorption peaks due to the transition between different LLs. At $E_0 = 10$ kV/cm, the full calculation (red curves) and the perturbation theory (gray curves) obviously differ around the first two peaks. This is not surprising because the perturbation theory fails for field stronger than 3 kV/cm. When the driving field is increased to $E_0 = 20$ kV/cm, the full calculation of the probe conductivity does not have any similarity to the perturbation results, and all peaks are greatly smeared out. This is consistent with the change of the selection rules and the occupations of LLs, which leads to a complicated behavior. For $E_0 = 51$ kV/cm, most of these peaks disappear, and a peak at very low frequency emerges. The spectra look very similar to the optical conductivity for a doped graphene at high temperature, indicating a fully thermalization of the electrons by the driving field. Because this system includes many energy scales, the probe conductivities do not depend on the driving field in a simple way, and their peaks can not be simply understood by side band effects.

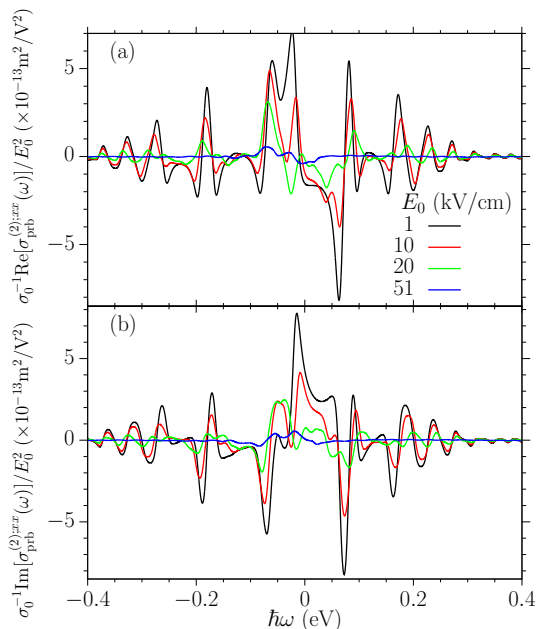


FIG. 4. (color online) The spectrum of the probe conductivity $\sigma_{\text{prb}}^{(0);xx}(\omega)$ for different driving fields with (a) the real part (b) the imaginary part.

The detection can also be made for frequencies $\omega \pm 2\Omega$, which correspond to the conductivity $\sigma_{\text{prb}}^{(\pm 2);xx}(\omega)$ for FWM. The results are shown in Fig. 4. At weak

driving fields, they recover the perturbative conductivities $\sigma_{\text{prb}}^{(2);xx}(\omega) = \sigma^{(3);xxxx}(\Omega, \Omega, \omega)$ and $\sigma_{\text{prb}}^{(-2);xx}(\omega) = [\sigma^{(3);xxxx}(\Omega, \Omega, -\omega)]^*$. The perturbative results agree very well with the conductivities at $E_0 = 1$ kV/cm. With increasing the field strength, the probe conductivities differ from the perturbative ones obviously, which are induced by the influences of the driving field on the system.

IV. CONCLUSION

In this study of the optical response induced by an intense periodic field, we constructed a theoretical framework based on the Floquet theorem, and derived the expressions for the full induced optical current. These expressions were used to study graphene subject to a strong perpendicular magnetic field. By comparing with a perturbation theory up to the third order, we determined the threshold field where the perturbation theory broke down. We understood these nonperturbative behavior from the Floquet states, which could be detected by a weak light field in an optical method. Our results can be extended to other systems.

There exist two unsolved issues in this approach: one is related to the driving field. Because most strong incident fields are laser pulses, they cannot be treated by a formalism based on fully periodic fields in a straightforward way. It would be necessary to extend the Floquet theorem to pulsed fields, even if appropriate approximations were required. The other is related to the phenomenological relaxation time approximation used in Eq. (2). As a widely adopted approximation in perturbation theory for preliminary studies, it is not clear whether or not it can be used, or how it would be implemented for very strong fields. Although a microscopic treatment of the scattering is possible,^{6,26} it would still be desirable to develop simpler descriptions that might lead to more physical insight.

ACKNOWLEDGMENTS

This work has been supported by CIOMP Y63032G160, CAS QYZDB-SSW-SYS038, and NSFC 11774340. J.L.C acknowledges valuable discussions with Prof. K. Shen and Prof. J.E. Sipe.

-
- ¹ M. O. Goerbig, *Rev. Mod. Phys.* **83**, 1193 (2011).
² K. M. Rao and J. E. Sipe, *Phys. Rev. B* **86**, 115427 (2012).
³ X. Yao and A. Belyanin, *Phys. Rev. Lett.* **108**, 255503 (2012).
⁴ X. Yao and A. Belyanin, *J. Phys. Condens. Matter* **25**, 054203 (2013).
⁵ J. C. König-Otto, Y. Wang, A. Belyanin, C. Berger, W. A. de Heer, M. Orlita, A. Pashkin, H. Schneider, M. Helm, and S. Winnerl, *Nano Lett.* **17**, 2184 (2017).
⁶ S. Brem, F. Wendler, and E. Malic, *Phys. Rev. B* **96**, 045427 (2017).
⁷ J. L. Cheng and C. Guo, arXiv:1711.04408 (2017).
⁸ M. Tokman, X. Yao, and A. Belyanin, *Phys. Rev. Lett.* **110**, 077404 (2013).
⁹ J. Shiri and A. Malakzadeh, *Laser Phys.* **27**, 016201 (2017).
¹⁰ W.-X. Yang, A.-X. Chen, X.-T. Xie, S. Liu, and S. Liu, *Sci. Rep.* **7**, 2513 (2017).
¹¹ G. Solookinejad, *Phys. B* **497**, 67 (2016).
¹² H. R. Hamed and S. H. Asadpour, *J. Appl. Phys.* **117**, 183101 (2015).
¹³ J. H. Shirley, *Phys. Rev.* **138**, B979 (1965).
¹⁴ F. J. López-Rodríguez and G. G. Naumis, *Phys. Rev. B* **78**, 201406 (2008) ; *Phys. Rev. B* **79**, 049901 (2009).
¹⁵ H. L. Calvo, H. M. Pastawski, S. Roche, and L. E. F. F. Torres, *Appl. Phys. Lett.* **98**, 232103 (2011).
¹⁶ M. Sentef, M. Claassen, A. Kemper, B. Moritz, T. Oka, J. Freericks, and T. Devereaux, *Nat. Commun.* **6**, 7047 (2015).
¹⁷ J. Cayssol, B. Dra, F. Simon, and R. Moessner, *Phys Status Solidi - Rapid research letters* **7**, 101 (2013).
¹⁸ X. G. Xu, S. Sultan, C. Zhang, and J. C. Cao, *Appl. Phys. Lett.* **97**, 011907 (2010).
¹⁹ Y. Zhou and M. W. Wu, *Phys. Rev. B* **83**, 245436 (2011).
²⁰ L. E. F. Foa Torres, P. M. Perez-Piskunow, C. A. Balseiro, and G. Usaj, *Phys. Rev. Lett.* **113**, 266801 (2014).
²¹ A. Kundu, H. A. Fertig, and B. Seradjeh, *Phys. Rev. Lett.* **113**, 236803 (2014).
²² A. P. Jauho and K. Johnsen, *Phys. Rev. Lett.* **76**, 4576 (1996).
²³ O. V. Kibis, S. Morina, K. Dini, and I. A. Shelykh, *Phys. Rev. B* **93**, 115420 (2016).
²⁴ M. Torres and A. Kunold, *Phys. Rev. B* **71**, 115313 (2005).
²⁵ Equation (9) gives $\sum_{n_1 n_2} eE_{\text{drv}}^{(n_1);d} \hat{\xi}^d u_{\alpha}^{(n_2)} [u_{\alpha}^{(n_1+n_2)}]^{\dagger} = \sum_l (l\hbar\Omega + \epsilon_{\alpha} - \hat{H}_0) u_{\alpha}^{(l)} [u_{\alpha}^{(l)}]^{\dagger}$. By substituting this expression into the numerator of Eq. (12), it can be simplified to $[\hat{H}_0, \hat{\rho}_0]$, which is zero.
²⁶ J. H. Jiang and M. W. Wu, *Phys. Rev. B* **75**, 035307 (2007).